Injectable protease-operated depots of glucagon-like peptide-1 provide extended and tunable glucose control

Miriam Amiram[a], Kelli M. Luginbuhl[a], Xinghai Li[a], Mark N. Feinglos[b], and Ashutosh Chilkoti[a,1]

[a]Department of Biomedical Engineering, Duke University, Durham, NC 27708-0281; and [b]Division of Endocrinology, Metabolism, and Nutrition, Duke University Medical Center, Durham, NC 27710

Edited by David A. Tirrell, California Institute of Technology, Pasadena, CA, and approved December 28, 2012 (received for review August 22, 2012)

Peptide drugs are an exciting class of pharmaceuticals increasingly used for the treatment of a variety of diseases; however, their main drawback is a short half-life, which dictates multiple and frequent injections and an undesirable "peak-and-valley" pharmacokinetic profile, which can cause undesirable side-effects. Synthetic prolonged release formulations can provide extended release of biologically active native peptide, but their synthetic nature can be an obstacle to production and utilization. Motivated by these limitations, we have developed a new and entirely genetically encoded peptide delivery system—Protease Operated Depots (PODs)—to provide sustained and tunable release of a peptide drug from an injectable s.c. depot. We demonstrate proof-of-concept of PODs, by fusion of protease cleavable oligomers of glucagon-like peptide-1, a type-2 diabetes drug, and a thermally responsive, depot-forming elastin-like-polypeptide that undergoes a thermally triggered inverse phase transition below body temperature, thereby forming an injectable depot. We constructed synthetic genes for glucagon-like peptide-1 PODs and demonstrated their high-yield expression in *Escherichia coli* and facile purification by a nonchromatographic scheme we had previously developed. Remarkably, a single injection of glucagon-like peptide-1 PODs was able to reduce blood glucose levels in mice for up to 5 d, 120 times longer than an injection of the native peptide drug. These findings demonstrate that PODs provide the first genetically encoded alternative to synthetic peptide encapsulation schemes for sustained delivery of peptide therapeutics.

drug delivery | sustained release | peptide polymers

With more than 40 approved peptide drugs worldwide and over 650 peptides in clinical and preclinical development, the field of peptide therapeutics is booming (1); with properties of high specificity, high activity, and rapid tissue penetration, peptides are particularly attractive as potential pharmaceuticals (2). Unfortunately, a major barrier to their clinical adoption stems from the fact that parenteral injection is the most effective route of peptide drug administration (3), but it leads to rapid clearance, which in turn requires frequent injections, leading to a "peak-and-valley" pharmacokinetic profile that can cause undesirable side-effects (4) and reduce patient compliance. In addition, other limitations of peptide drugs are their poor stability, costly production, and proteolytic susceptibility. An ideal peptide drug delivery system would hence solve these problems by providing prolonged release of native, stable, and biologically active peptide while limiting injection frequency. Injectable prolonged release formulations of peptides have been developed that use biodegradable microparticles as depots, but they suffer from several important limitations in scale-up and manufacturing such as a complex production and formulation process that requires a chemically synthesized peptide to be loaded into a biodegradable polymer microparticle while maintaining tight control on peptide loading, microparticle size, and morphology without compromising the activity of the peptide drug and the sterility of the final product.

Herein, we describe a completely genetically encodable peptide depot with no synthetic components that we term Protease Operated Depot (POD) that attempts to solve these problems. A POD consists of two components that are fused together at the gene level and recombinantly expressed as one continuous polypeptide: (*i*) oligomers of a peptide drug with recognition sites for an in vivo protease that are embedded between the peptide repeats and (*ii*) a thermally sensitive elastin-like polypeptide (ELP) that is soluble at room temperature but forms a depot—a viscous coacervate—upon s.c. injection at body temperature (5). The central hypothesis that underlies the design of PODs is that the ELP will trigger a thermal phase transition upon s.c. injection, thereby forming a stable drug depot. Over time, active peptide will be released by protease cleavage between copies of the peptide, providing prolonged release of bioactive drug into circulation (Fig. 1*A*).

For proof-of-principle of PODs, we focused on type-2 diabetes, a disease with an enormous and unmet clinical need, with a forecast of 300 million patients globally by 2025 (6). We chose glucagon-like peptide-1 (GLP-1) as the drug because incretin mimetics, peptide analogs of the naturally occurring GLP-1, are an exciting new class of type-2 diabetes drugs with numerous antihyperglycemic activities on various organs (7). GLP-1 is a 30 amino acid peptide released by gastrointestinal cells in response to meal ingestion (8) (Fig. S1), which has been found to be beneficial for the treatment of type-2 diabetes primarily by stimulating the release of insulin from pancreatic β-cells (9). In addition, GLP-1 has also been shown to inhibit glucagon secretion, reduce appetite, slow gastric emptying, reduce hepatic glucose production (10, 11), and enhance β-cell survival and growth in rodents (12). Unlike insulin and other insulin secretagogues (such as sulfonylureas), which act independently of glucose level and therefore increase the risk for hypoglycemia, the insulinotrophic effects of GLP-1 are glucose dependent and vanish when glucose levels drop below 60 mg/dL, preventing potentially life-threatening hypoglycemia (13). Despite these attractive pharmacological features, native GLP-1 has not been used for treatment of type-2 diabetes because the peptide undergoes rapid deactivation in vivo via N-terminal truncation by dipeptidyl-peptidase IV (DPPIV), leading to an in vivo half-life of less than 2 min (14). To circumvent this problem, DPPIV-resistant GLP-1 analogs have been proposed. However, due to the small size of these GLP-1 analogs, renal clearance still limits the half-life to 4–5 min (14), so that clinically approved formulations of GLP-1 mimetics such as exenatide—a 39 amino acid peptide derived from the Gila monster that has 53% homology to GLP-1—require twice daily injections and cause side-effects such as nausea (15). Hence, a controlled release system of GLP-1 that minimizes injection frequency and

Author contributions: M.A. and A.C. designed research; M.A., K.M.L., and X.L. performed research; M.A., M.N.F., and A.C. analyzed data; and M.A. and A.C. wrote the paper.

Conflict of interest statement: A.C. is cofounder of a start-up company, PhaseBio Pharmaceuticals, in Malvern, PA, that is commercializing elastin-like polypeptides for applications in biotechnology and medicine.

This article is a PNAS Direct Submission.

[1]To whom correspondence should be addressed. E-mail: chilkoti@duke.edu.

This article contains supporting information online at www.pnas.org/lookup/suppl/doi:10.1073/pnas.1214518110/-/DCSupplemental.

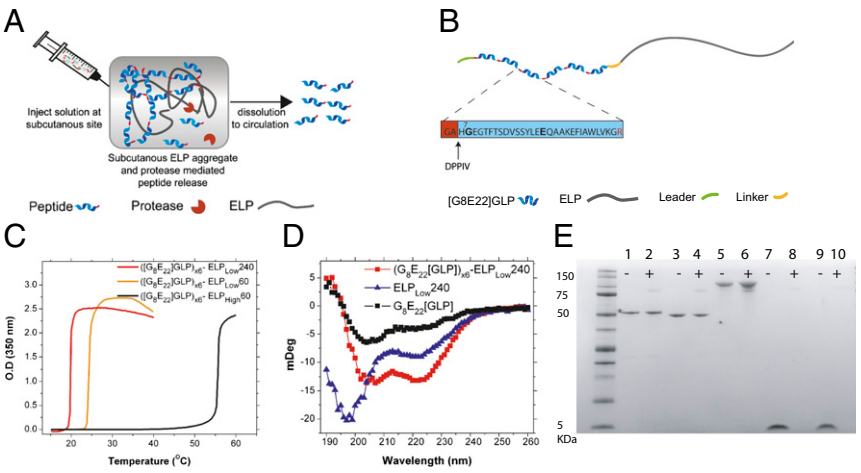

Fig. 1. Design and characterization of GLP-1 PODs. (*A*) Soluble fusion proteins of $(peptide)_n$-ELP are injected s.c. and coacervate in situ in response to body temperature to form a depot. Subsequently, s.c. proteases release active peptide into circulation. (*B*) The final—optimized—GLP-1 POD construct includes a short leader peptide, followed by 6 [G8E22]GLP monomers, a trailer peptide, and an ELP. The GLP-1 monomers were mutated at position 8 (alanine to glycine) to confer DPPIV resistance and position 22 (glycine to glutamic acid) to stabilize the α-helical secondary structure of GLP-1. A GA dipeptide was added to each GLP-1 N terminus to generate an arginine-glycine protease cleavage site between neighboring monomers in the POD. The GA dipeptide in the monomer that is liberated after cleavage by an arginine-specific protease in the s.c. space is a substrate for DPPIV, a ubiquitous exopeptidase that cleaves off this dipeptide, thereby liberating the active GLP-1 monomer. We note that DPPIV is normally implicated in the in vivo deactivation of native GLP-1 but that here, cleavage by the enzyme serves to activate the GLP-1 N terminus rather than to deactivate it. (*C*) Transition temperature of $([G8E22]GLP)_{x6}$ fused to ELPs of varying hydrophobicity and molecular weight at a concentration of 150 μM. (*D*) CD spectra of monomer $[G_8E_{22}]GLP$ (15 μM), $ELP_{Low}240$ (2.5 μM), and $([G_8E_{22}]GLP)_{x6}$-$ELP_{Low}240$ (2.5 μM fusion protein or 15 μM GLP-1 equivalents). (*E*) Degradation of PODs, non-depot-forming soluble fusions, or GLP-1 by NEP after 18 h incubation at 37 °C. Lane 1, $([G_8E_{22}]GLP)_{x6}$-$ELP_{High}60$; lane 2, $([G_8E_{22}]GLP)_{x6}$-$ELP_{High}60$+NEP; lane 3, $([G_8E_{22}]GLP)_{x6}$-$ELP_{Low}60$; lane 4, $([G_8E_{22}]GLP)_{x6}$-$ELP_{Low}60$+NEP; lane 5, $([G_8E_{22}]GLP)_{x6}$-$ELP_{Low}240$; lane 6, $([G_8E_{22}]GLP)_{x6}$-$ELP_{Low}240$ +NEP; lane 7, $[G_8E_{22}]GLP$; lane 8, $[G_8E_{22}]GLP$ +NEP; lane 9, native GLP-1; lane 10, native GLP-1+NEP. NEP may be seen as a faint band at ∼85 kDa.

provides sustained release of the peptide over time with the potential to minimize the spike in GLP-1 levels that is typical for injection of soluble peptide is highly desirable (16).

With this rationale in mind, we describe the construction of GLP-1 PODs and their utility in reducing glucose levels for 5 d following a single s.c. injection in mice. We show that PODs are easily expressed in high yields in *Escherichia coli* and that ELP fusion tags enable temperature-triggered coacervation that is tunable by choice of the ELP, allowing for facile, chromatography-free protein purification (17, 18). We demonstrate that PODs allow for protease-mediated GLP-1 release from the s.c. depot that provides vastly superior glucose control compared with injection of the monomer peptide.

Results

The nomenclature we use in the paper is as follows: All GLP-1 mutants throughout this paper are derived from the native GLP-1 [7–36], which is processed in vivo by cleavage of residues 1–6 (19) (Fig. S1) (20). PODs are designated $([Y]GLP)_{xN}$-ELP_SABC, where Y refers to the mutation in the sequence of GLP-1, N is the number of GLP-1 repeats, and the subscript s is either low, denoting an ELP designed to form a depot in vivo by selecting Valine (V) as fourth guest residues in the pentapeptide repeat, or high, denoting an ELP that has a T_t above body temperature, by alternating the guest residue between Glycine (G) and Alanine (A) residues. The subscript ABC refers to the number of VPGXG pentapeptide repeats. For example, $([G8E22]GLP)_{x6}$-$ELP_{Low}60$ refers to six repeats of the G8E22 mutant of GLP-1 that is fused to an ELP with 60 VPGXG repeats with a T_t that is below body temperature, so that this construct would undergo coacervation upon s.c. injection and form a POD in vivo. In contrast, the equivalent "high" construct is identical in all respects, except that it contains a different—more hydrophilic—ELP sequence so that its T_t is greater than body temperature and it hence remains soluble upon s.c. injection and does not form a POD.

We synthesized a library of GLP-1 oligomers wherein a number of variables were systematically explored: (*i*) number of GLP-1 repeats, (*ii*) their amino acid composition (14), and (*iii*) the sequence of the intervening protease cleavage site (21). This library consisted of genes for five different GLP-1 variants, for which oligomers of different lengths were generated, which could then be fused with three different ELPs leading to a potential pool of 75 unique POD designs (Table S1). A subset of these PODs were screened for expression yield and structural stability.

Based on these preliminary scouting studies, we designed an optimized POD with a therapeutic payload that has the following features. First, we chose a GLP-1 analog—$[G_8E_{22}]GLP$—that has an alanine (A) to glycine (G) substitution at residue 8 to confer DPPIV resistance and a glycine (G) to glutamic acid (E) substitute at residue 22 (14) to stabilize its α-helical structure. Second, a glycine-alanine (GA) dipeptide was added to the N terminus of each GLP-1 unit to introduce a protease cleavable arginine (R)–glycine (G) pair between successive peptides. This dipeptide can be cleaved by DPPIV in vivo to liberate the native N-terminal histidine (H) of GLP-1, so that, in our POD design, DPPIV serves to activate GLP-1 instead of its customary biological role of deactivating GLP-1. A monomer of this GLP-1 analog, which includes a "GA" dipeptide leader, termed [G8E22]GLP throughout the paper, was synthesized by AnaSpec and used as a control for all in vivo efficacy studies (for full sequence details, see Table S1). Third, because dimers of GLP-1 and its analog, exenatide (trade name Byetta), have been shown to activate GLP-1R (16, 22), a protective leader peptide (Table S1) was incorporated at the N terminus of the POD to ensure that the activity does not ensue from release of intact fusion protein from the depot; this peptide has a C-terminal arginine (R) to ensure its cleavage in vivo. Finally, we chose 6× GLP-1 oligomers (GLP_{x6}) as the payload because it provides an optimal balance between high expression level and high drug loading (Fig. 1*B*).

The depot-forming ELP that is the second component of the POD was optimized concurrently. ELPs are a family of thermally responsive peptide polymers composed of a VPGXG repeat that is derived from a recurring pentapeptide motif that is found in tropoelastin (17). ELPs are soluble in aqueous solutions below their inverse transition temperature (T_t) but undergo a sharp (∼2 °C range) phase transition when the temperature is raised above their T_t, leading to the formation of an ELP-rich coacervate phase. The ELP phase transition has been extensively characterized, allowing us to precisely tune its thermal phase transition behavior (5) (Table S1), which enables us to inject a POD as a low viscosity solution (23) that undergoes its phase transition in vivo upon s.c. injection to form a depot. Importantly, the ELP can be fused at the gene level to GLP-1 oligomers and recombinantly expressed as a single polypeptide chain and expressed in *E. coli* (18).

Production of all GLP_{x6} PODs used an Isopropyl β-D-1-thiogalactopyranoside (IPTG) induction protocol in *E. coli*. The fused ELP component of PODs enabled their facile, chromatography-free purification by inverse transition cycling (ITC) (Fig. S2) (24), with yields of ~150 mg/L of purified PODs in a shaker flask culture. By tuning the composition of the ELP, we were able to create GLP-1 PODs with a T_t below body temperature (POD forming, ELP_{Low}) or above body temperature (soluble control, ELP_{High}) (Fig. 1*C*). The T_t—the coacervation temperature of the fusion—was controlled by varying the ELP hydrophobicity and M_r, and all PODs displayed a typical, sharp transition at their T_t that is experimentally observed as a large increase in the turbidity of the POD solution at the T_t. Although some GLP-1 variants displayed an irreversible transition profile due to structural changes (25), $([G_8E_{22}]GLP)_{x6}$ PODs were completely resolubilized upon cooling below their T_t (Fig. S3 *A–C*). $([G_8E_{22}]GLP)_{x6}$ PODs also maintained α-helical secondary structure compared with the highly disordered structure of the ELP, as indicated by their circular dichroism (CD) spectra (14) (Fig. 1*D*, Fig. S3 *D* and *E*). We also found that PODs are far more resistant than GLP-1 monomers to degradation by neutral endopeptidase (NEP), a protease known to degrade GLP-1 in vivo (26). Both depot-forming PODs and soluble fusion controls were resistant to NEP degradation at temperatures below (16 °C) and above (37 °C, body temperature) their transition, suggesting that premature degradation of PODs in the s.c. space is likely to be minimized (Fig. 1*E*, Fig. S4). Since both the depot forming PODs and the soluble fusion—negative control—constructs are resistant to degradation by NEP (at 16 and 37 °C), this resistance is likely due to the unstructured ELP polymer chain that creates steric hindrance between NEP and its degradation sites in GLP-1.

We assessed the in vitro release of GLP-1 by incubation of PODs with the arginine-specific protease, Factor X (FXa), followed by a GLP-1 receptor (GLP-1R) activation assay. While even high (1 μM) concentrations of intact $([G_8E_{22}]GLP)_{x6}$-$ELP_{Low}240$ PODs could not activate the GLP-1R (compared with $EC_{50} = 0.23$ nM of

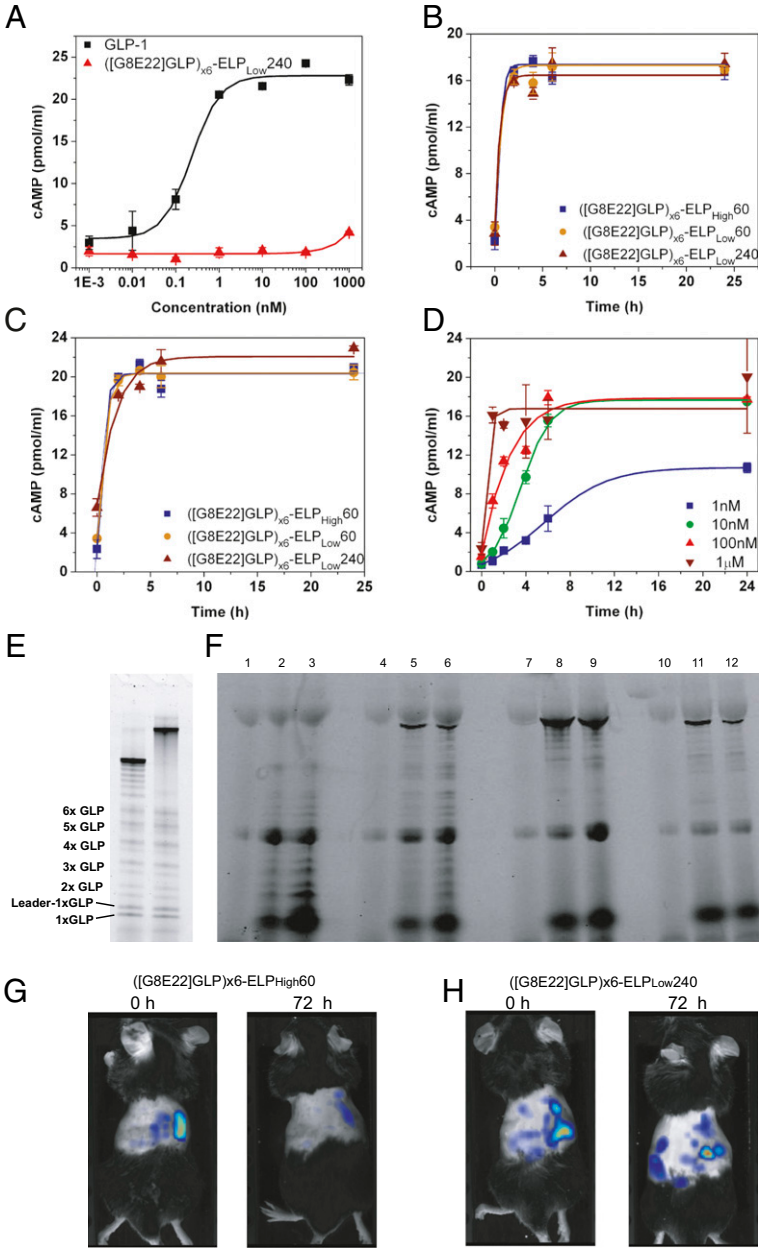

Fig. 2. In vitro and in vivo activation of GLP-1 PODs. (*A*) cAMP response of native GLP vs. nonactivated $([G_8E_{22}]GLP)_{x6}$-$ELP_{Low}240$ PODs in BHK cells expressing the GLP-1R. (*B* and *C*) cAMP response of 1 μM each of $([G_8E_{22}]GLP)_{x6}$-$ELP_{Low}240$, $([G_8E_{22}]GLP)_{x6}$-$ELP_{Low}60$ PODs, and $([G_8E_{22}]GLP)_{x6}$-$ELP_{High}60$ soluble control activated by cleavage with the arginine-specific protease, FXa, for 0, 2, 4, 6, and 24 h at 37 °C (*B*) and 16 °C (*C*). (*D*) cAMP response of $([G_8E_{22}]GLP)_{x6}$-$ELP_{Low}240$ at 1,10,100 nM, and 1 μM activated by cleavage with the arginine-specific protease, FXa, for 0, 2, 4, 6, and 24 h at 16 °C. (*E*) Proteolysis products of $([G_8E_{22}A_{36}]GLP)_{x6}$-$ELP_{Low}60$ (lane 1) and $([G_8E_{22}]GLP)_{x6}$-$ELP_{Low}240$ (lane 2) after incubation with FXa. Released GLP-1 and GLP-1 oligomers are seen as doublets representing GLP-1 concatemers with and without the protective leader peptide as confirmed by protein sequencing of several bands. (*F*) SDS/PAGE gel of Dylight 488–labeled PODs, injected s.c. and sampled from the tail vain at 0, 3, and 6 h postinjection. $([G_8E_{22}]GLP)_{x6}$-$ELP_{Low}240$ at 0, 3, and 6 h postinjection (lanes 1, 2, and 3, respectively); $([G_8E_{22}]GLP)_{x6}$-$ELP_{Low}60$ at 0, 3, and 6 h postinjection (lanes 4, 5, and 6, respectively); $([G_8E_{22}]GLP)_{x6}$-$ELP_{High}60$ at 0, 3, and 6 h postinjection (lanes 7, 8, and 9, respectively); and $([G_8E_{22}A_{36}]GLP)_{x6}$-$ELP_{Low}60$ without C-terminal arginine at 0, 3, and 6 h postinjection (lanes 10, 11, and 12, respectively). (*G* and *H*) NIR tomography images after a single s.c. injection of (*G*) $([G8E22]GLP)_{x6}$-$ELP_{High}60$ and (*H*) $([G8E22]GLP)_{x6}$-$ELP_{Low}240$ immediately following (0 h) and 72 h after s.c. injection.

native GLP-1; Fig. 2*A*), GLP-1 released from 1 μM PODs after incubation with FXa at both 37 °C and 16 °C was able to fully activate the GLP-1R (Fig. 2 *B* and *C*). Further, we attempted to simulate the protease-triggered "dose-response" of GLP-1 release from a POD as a function of concentration of the parent construct—$([G_8E_{22}]GLP)_{x6}$-$ELP_{Low}240$. This experiment was carried out by incubating 1 nM – 1 μM of $([G_8E_{22}]GLP)_{x6}$-$ELP_{Low}240$ POD with FXa at 16 °C; we chose 16 °C for this experiment because it is below the T_t of $([G_8E_{22}]GLP)_{x6}$-$ELP_{Low}240$ at all of the concentrations that span the experiment. As expected, increasing the concentration of $([G_8E_{22}]GLP)_{x6}$-$ELP_{Low}240$ POD caused an increase in GLP-1 released by FXa and thus an increase in the observed cAMP concentration (Fig. 2*D*). Cleavage of the PODs incubated with FXa was confirmed by SDS/PAGE, protein sequencing, and MALDI-TOF analysis of the GLP-1 oligomer bands (Fig. 2*E*, Fig. S5).

To validate protease-mediated s.c. "activation," PODs were labeled with Dylight 488 on their lysine residues, injected s.c., and blood fractions were analyzed by SDS/PAGE for fluorescent protein bands. In vivo, thermally reversible PODs designed to form a depot following injection exhibit a similar cleavage pattern as seen in vitro (Fig. S6). Notably, the size of the ELP affected the release of intact fusion proteins from the s.c. site of injection: intact $([G_8E_{22}]GLP)_{x6}ELP_{Low}60$ is clearly observed in blood, whereas intact $([G_8E_{22}]GLP)_{x6}$-$ELP_{Low}240$ is barely observed (Fig. 2*D*, lanes 1–6), and only intact soluble $([G_8E_{22}]GLP)_{x6}$-$ELP_{High}60$ is rapidly released to circulation (Fig. 2*D*, lanes 7–9), thus reinforcing the hypothesis that the primary site of protease mediated GLP-1 release is within the s.c. depot and not in systemic circulation. Additionally, only intact fusion protein is released from a control POD, $([G_8E_{22}A_{36}]GLP)$-$ELP_{Low}60$ (Table S1), in which the arginine-specific protease cleavage site was eliminated (Fig. 2*E*, lanes 10–12), thus supporting the notion that proteolytic cleavage at arginine residues within the s.c. space is responsible for release of GLP-1 from the POD. Upon careful observation, some faint bands are visible below all intact fusion proteins, which may indicate some degradation in plasma or s.c.; however, the low relative intensity of these bands indicates that nonspecific degradation of the POD is low compared with the engineered arginine cleavage and release of GLP-1.

To visualize depot formation in vivo, NIR (near infrared)-labeled PODs and a soluble control were injected s.c. and imaged for up to 1 wk postinjection. Fluorescence tomography images show that the size of depots created by both $([G8E22]GLP)_{x6}$-$ELP_{Low}60$ and $([G8E22]GLP)_{x6}$-$ELP_{Low}240$ PODs was larger than for the soluble control, $([G8E22]GLP)_{x6}$-$ELP_{High}60$. The soluble control had also largely dissipated by 72 h postinjection (Fig. 2*F*), while the $([G8E22]GLP)_{x6}$-$ELP_{Low}240$ POD was clearly visible at 72 h postinjection (Fig. 2*G*) and persisted for over 5 d (Figs. S7–S9).

After confirmation of the formation of a stable depot after s.c. injection and subsequent proteolytic release of active GLP-1 monomers from the PODs, we next sought to determine whether a single s.c. injection of a POD could provide reduction of glucose levels over an extended period. A single s.c. injection of several different designs of PODs (11 nmol/mouse) were administered to mice and fed glucose levels were monitored for up to 1 wk postinjection. We found that PODs were able to significantly extend the glucose-lowering effect of GLP-1. While the $([G_8E_{22}]GLP)_{x6}$-$ELP_{Low}60$ POD that has an ELP with a M_r of 25 KDa provided extended glucose reduction for up to 48 h (ANOVA $P < 0.001$, Fig. 3*A*), the larger $([G_8E_{22}]GLP)_{x6}$-$ELP_{Low}240$ POD with an ELP M_r of 100 KDa reduced glucose for up to 120 h (ANOVA $P < 0.001$, Fig. 3*B*). These results are in stark contrast with the very temporally limited activity of [G8E22]GLP monomer (1 nmol/mouse) that only lowers glucose levels for 1 h following s.c. injection (Fig. 3*C*). The importance of forming a POD is clear from the observation that the $([G_8E_{22}]GLP)_{x6}$-$ELP_{High}60$ construct that does not form a depot but instead remains soluble upon s.c. injection only showed a minor and transient reduction in glucose levels that only lasted for the first 6 h postinjection (Fig. 3*D*).

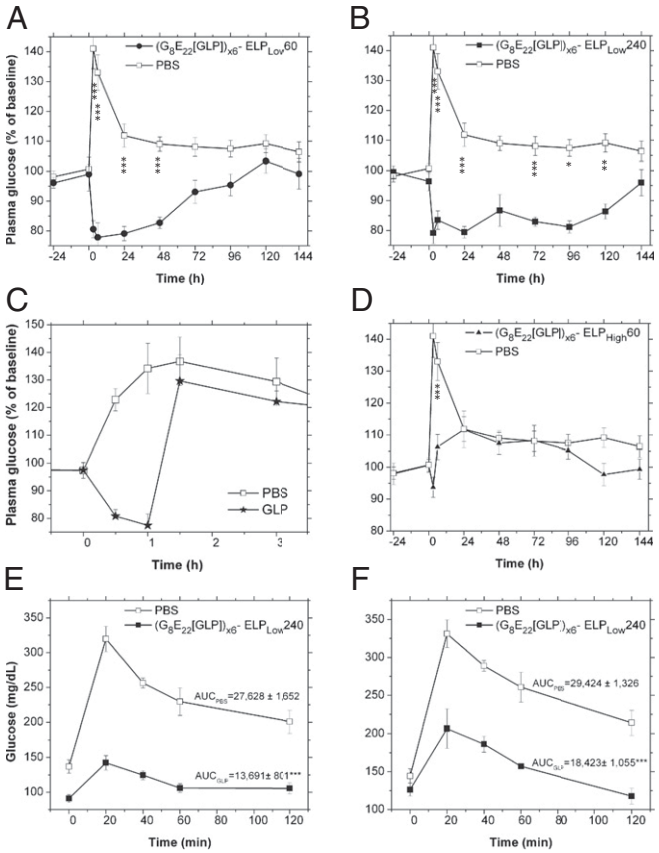

Fig. 3. Prolonged in vivo glucose reduction following a single injection of PODs. (*A–D*) Daily fed blood glucose levels before and after a single s.c. injection of (*A*) $([G8E22]GLP)_{x6}$-$ELP_{Low}60$, (*B*) $([G_8E_{22}]GLP)_{x6}$-$ELP_{Low}240$, (*C*) $[G_8E_{22}]GLP$, and (*D*) $([G_8E_{22}]GLP)_{x6}$-$ELP_{High}60$ (all POD constructs injected at 11 nmol/mouse, monomer $[G_8E_{22}]GLP$ injected at 1 nmol/mouse). Injection was administered at the 0 h time point. $*P < 0.05$, $**P < 0.01$, $***P < 0.001$. (*E* and *F*) IPGTT following a single injection of $([G8E22]GLP)_{x6}$-$ELP_{Low}240$. Blood glucose levels in 7-wk-old mice during IPGTT performed at (*E*) 52 h and (*F*) 102 h after an injection of $([G8E22]GLP)_{x6}$-$ELP_{Low}240$ (11 nmol/mouse, $***P < 0.001$).

To validate these results, an i.p. glucose tolerance test (IPGTT) was performed 54 h and 102 h after a single injection of $([G8E22]GLP)_{x6}$-$ELP_{Low}240$ PODs (11 nmol/mouse). IPGTT confirmed the presence of GLP-1 and its significant effect on glucose clearance: at 54 h postinjection, the area under the curve (AUC) is reduced by 50% ($P < 0.001$, Fig. 3*E*), and at 102 h postinjection, AUC is reduced by 37% for treated mice compared with PBS-treated controls ($P < 0.001$, Fig. 3*F*).

Discussion

There are conceptually two strategies to improve the bioavailability and efficacy of peptide drugs such as GLP-1 and its analogs. One strategy employs peptide fusion to large molecular weight carriers such as plasma proteins (27, 28), biopolymers (29), or soluble synthetic polymers (14). However, large fusion proteins interfere with receptor binding causing significant loss in efficacy (14, 27) and can require expensive eukaryotic expression systems or low-yield nonspecific chemical conjugations and expensive and complicated postconjugation separation of the product from residual reactants.

The second approach to improve bioavailability and efficacy involves the release of a peptide drug from an implanted or injected sustained release device. In the case of GLP-1, Bydureon, a sustained release formulation of exenatide entrapped in biodegradable

poly(lactic glycolic acid) (PLGA) microspheres, was recently approved for once-weekly injection in humans (30). There are two important advantages to sustained release formulations: the native, fully active peptide is released and a broad range of release profile can be designed by modifying the properties of the release formulation. However, despite these advantages, microsphere encapsulation formulations suffer significant drawbacks that mainly result from their synthetic nature. First, the dose required by Bydureon is 14–28-fold larger compared with exenatide (31), exemplifying the fact that microsphere optimization is difficult and in vivo behavior can be unpredictable. Second, their preparation requires separate synthesis of the peptide and polymer and coformulation into microspheres of a precise size, a complex process that must be carried out in a sterile environment (3). Third, sustained release polymer microsphere suspensions are viscous and hence require painful injections with large gauge needles. Fourth, degradation of PLGA can cause fibrosis (32). Finally, peptide bioavailability may also be significantly reduced due to peptide adsorption to the polymer matrix and denaturation of the peptide (33).

Although there are many reports of peptide conjugation to both proteins and synthetic polymers, to the best of our knowledge, there have been no attempts to mimic synthetic microsphere technologies using an entirely genetically encoded system. We therefore sought to design such a system—PODs—that we believe provides a simple and elegant solution that circumvents the limitations of current synthetic prolonged release formulations. We administered PODs at 11 nmol/mouse or 66 nmol GLP-1 equivalents/mouse compared with 1 nmol/mouse injection of DPPIV-resistant GLP monomer administered by us and others (34). Thus, assuming a best case scenario of 4-h glucose control by monomer GLP-1 (shown in ref. 34) and a worst case scenario of 1.5 h for the same mutant of GLP-1 as used in the POD (Fig. 3*C*), the cumulative dose to maintain the same level of glucose control would require 30 injections (compared with a single POD injection) leading to a dose of 30 nmol/mouse (assuming 4 h glucose control) or 80 nmol/mouse (assuming 1.5 h glucose control) over the course of 5 d. Thus, the dose required by PODs is only ~twofold higher at worse and less than 1.2-fold lower at best than the cumulative dose of monomer GLP-1, which compares favorably with the 14–28-fold dose inefficiency of Bydureon. This loss is also dwarfed, in our opinion, by the significant reduction in the number of injections required.

In addition, in contrast to the complicated scale-up process in microsphere production, GLP-1 PODs are genetically encoded as a single polypeptide, exhibit high expression levels even in shaker flask culture in *E. coli*, and can be easily purified by the phase transition behavior imparted to a POD by its ELP domain. Importantly, PODs are controlled by orthogonal design elements that can be manipulated at the gene level, and these elements allow the performance of the POD to be tuned in a predictable fashion. For example, we show that a POD with a short ELP (25 KDa) provides glucose control for 48 h, while a POD with a longer ELP (100 KDa) provides glucose control for 120 h. Because we have in hand a large set of diverse ELPs (17), we believe that with further optimization PODs could be tuned for even longer durations. Additionally, the design of the protease cleavage site between GLP-1 monomers can control the rate of peptide release. This degree of modularity and control is difficult to access with synthetic peptide encapsulation technologies, in our opinion.

Although these results are promising, we believe that a deeper understanding of the mechanism of GLP-1 POD activation in vivo is necessary to optimize PODs for clinical translation. Some inefficiency in using the full GLP-1 dose may be due to several reasons. First, the fraction of larger M_r bands corresponding to GLP-1 dimer and higher M_r oligomers seen in circulation are pharmacologically inactive and represent the fraction of the dose that is not bioavailable. This problem can be addressed by mutating the protease site between GLP-1 monomers to largely yield monomeric active GLP-1. Second, unidentified proteases may prematurely degrade the GLP-1 that is liberated from a POD in the s.c. compartment or in its transit to its site of action. Should this prove to be the case, the design of GLP-1 mutants that are more proteolytically stable than the native peptide may prevent this premature degradation. Future studies will focus on studying these issues.

Going forward, the modular and flexible genetically encoded design of PODs should, we believe, allow variations of this new peptide delivery system to provide capabilities that are unattainable with current microsphere technology. For example, next generation PODs will include protease cleavage sites that are not identical, but instead range from "slow" to "fast" in their cleavage kinetics, which will provide an additional level of temporal control over circulating levels of the peptide drug. More sophisticated designs could also involve a POD in which multiple peptide drugs—with a synergistic mode of action—are incorporated and loaded with different number of copies of each drug that are consistent with their required cumulative dose and with cleavage sites that are individually tailored to release each peptide drug at a rate that is optimized for its unique pharmacological profile.

Materials and Methods

GLP-1 Oligomer Gene Synthesis and POD Expression. Synthetic genes encoding GLP-1 oligomers and its mutants were assembled by Overlap Elongation Rolling Circle Amplification (OERCA), as previously described (21). Colonies with oligomers of $(GLP\text{-}1)_{x6}$ were selected from OERCA libraries and ligated to various ELP genes. The resulting POD constructs were expressed and purified using a modified ITC protocol (24) detailed in *SI Materials and Methods*.

Phase Transition and Secondary Structure Analysis. Secondary structures of PODs, soluble controls, and GLP-1 monomer were studied by CD spectroscopy using an Aviv Model 202 instrument and 1 mm quartz cells (Hellma) by scanning from 180 nm to 280 nm with 1 nm steps and a 3 s averaging time at 19 °C. Purified constructs were dialyzed overnight against Milli-Q water, and the solutions were diluted to 15 or 2.5 μM in water (monomer GLP-1 and PODs, respectively). Data were considered for analysis whenever the Dynode voltage was below 500 V (35).

To characterize the inverse transition temperature behavior of GLP-1 PODs and soluble controls, the optical density of a 150 μM solution in PBS was monitored at a wavelength of 350 nm as a function of temperature, with heating and cooling performed at a rate of 1 °C min^{-1} on a Cary 300 UV-visible spectrophotometer equipped with a multicell thermoelectric temperature controller (Varian Instruments).

Proteolysis of PODs. $([G8E22]GLP)_{x6}$-$ELP_{Low}240$ $([G8E22]GLP)_{x6}$-$ELP_{Low}60$ and $([G8E22]GLP)_{x6}$-$ELP_{High}60$ PODs (5 μM), [G8E22]GLP, and native GLP-1 (30 μM) were incubated at 16 °C or 37 °C for up to 18 h with 0.46 μg NEP protease (Enzo). Following incubation, fractions were separated on a 10–20% Tris-tricine SDS gel (Biorad) and stained with coomassie brilliant blue.

$([G8E22]GLP)_{x6}$-$ELP_{Low}240$ was incubated for 16–24 h with 1.1 μg FXa protease (Thermo Scientific) at 16 °C, and the resulting cleavage products were visualized on an SDS gel (NuPAGE, Invitrogen) and stained with coomassie brilliant blue. Several GLP-1 polymer bands were excised from the gel for protein sequencing (Duke Proteomics facility), and a 24-h cleaved sample was analyzed by MALDI-TOF to verify the M_r of the cleaved GLP-1 oligomers (Duke Proteomics facility).

In Vitro Assay for GLP-1 Activity. The ability of GLP-1 PODs to release GLP-1 monomers after incubation with 1.1 μg FXa protease (Thermo Scientific) and 0.5 μg DPPIV (ProSpec) and to activate the GLP-1 receptor (GLP-1R) in vitro was assessed using Baby Hamster Kidney (BHK) cells that are stably transfected with rat GLP-1R (a gift of Drucker, University of Toronto, Toronto, Canada) (36). Intracellular cAMP concentrations were measured using a competitive binding assay according to the manufacturer's instructions (Assay Designs).

Animal Studies. The 5–6-wk-old male C57BL/6J mice (37) (stock no. 000664) were purchased from Jackson Laboratories. All experimental procedures were approved by the Duke Institutional Animal Care and Use Committee.

Fluorescent Labeling and Imaging of in Vivo Release of GLP-1 from PODs. For in vivo visualization, PODs were fluorescently labeled with Dylight 488-NHS ester (Pierce) by conjugation to lysine residues in GLP-1. Labeled constructs were injected s.c. (11 nmol/mouse). Blood samples were withdrawn from the tail vain [10 μL in 100 μL 10% (vol/vol) heparin in PBS], and in vivo GLP-1

release from polymers were visualized by running on a 10–20% Tris-tricine SDS gel (Bio-Rad), and analysis of blood samples was performed by visualization of fluorescent protein bands at 488 nm with a Typhoon 9410 scanner.

In Vivo Near Infrared Fluorescence Tomography. For in vivo tomography of depot formation, PODs were labeled with IRDye 800CW NHS Ester (LICOR) by conjugation to lysine residues in GLP-1. All mice were anesthetized with 2% isoflurane throughout the imaging procedures. The torsos of mice (7 wk old, $n = 3$ per group) were shaved, and labeled constructs were injected s.c. (11 nmol/mouse). Images were collected immediately after injection and at 5, 24, 48, 72, 96, 120, and 144 h postinjection. Imaging was performed with an FMT2500LX fluorescence tomography in vivo imaging system (PerkinElmer), and the images were acquired and analyzed with TrueQuant 3D software (PerkinElmer). When depicted in the same panel, all image intensities were set to the maximum intensity scale of the first (0 h) image.

Fed Blood Glucose Measurements. The effect of GLP-1 PODs on fed blood glucose levels was measured following a single s.c. injection of a POD or soluble control. Before blood glucose measurement, the tail was wiped with a sterilizing alcohol solution and wiped dry. A tiny incision of the mouse tail vein was made, and the first 1 μL drop of blood was wiped off. The second 1–2 μL blood drop was measured by a glucose oxidase test, using a hand-held glucometer (AlphaTrack, Abbott, set to code 7). Blood glucose levels were measured at 3 d and 1 d before initiating the experiment. On the day of injection, animals were weighed, blood glucose was measured, and a POD solution (11 nmol/mouse, 3.5 μL/g, 13–17 °C) or PBS was injected s.c. ($n = 7$–11). Immediately following injection, mice were placed back in the cage, with free access to food and water, and blood glucose was measured at 3, 6, 24, 48, 72, 96, 120, 144, and 168 h after the injection. Blood glucose levels were normalized by the average glucose levels taken on the days before and immediately before injection to reflect the percent change in glucose levels and to correct for transient variations in glucose.

IPGTT. At the beginning of the experiment, mice were randomly divided into four groups ($n = 5$) based on two previous measurements of blood glucose. At 9:00 AM on the first day (time = 0), all mice were injected s.c. with $([G_8E_{22}]GLP)_{x6}$-$ELP_{Low}240$ PODs (11 nmol/mouse) or PBS. In the morning of the first IPGTT experiment (9:00 AM, 48 h following injection), two groups of mice (injected with either PODs or PBS control) were fasted by placement in a fresh cage and removal of food for 5 h. At the end of the fast period (52 h following injection), mice were given 1 g glucose/kg [10% (wt/vol) sterile glucose solution, Sigma] via i.p. injection. Blood was drawn from the tail vein, and glucose levels were measured using a glucometer at 0, 20, 40, 60, 90, and 120 min after glucose administration. On the morning of the second IPGTT experiment (9:00 AM, 97 h following injection), the two remaining groups of mice (injected with either PODs or PBS control) were subjected to the same protocol and an IPGTT was similarly performed (102 h following injection).

Data Analysis. Data are presented as means and SEs. Treatment effects on fed glucose levels were first analyzed using repeated measures ANOVA for all groups. When the initial analysis indicated a significant difference, lower order ANOVAs were conducted to determine the effects of each treatment, followed by post hoc evaluations of individual differences at each time point for treatment compared with the PBS control using Fisher's Protected Least Significant Difference. For AUC of IPGTT evaluation, treatment and PBS were compared using a one-tailed heteroschedastic t test.

ACKNOWLEDGMENTS. We thank the Duke University School of Medicine for the use of the Duke Proteomics Core Facility, which provided MALDI-TOF and protein sequencing services. A.C. acknowledges the financial support of National Institutes of Health Grant R01DK091789, and M.A. acknowledges the support of a graduate fellowship from the Center for Biologically Inspired Materials and Material Systems at Duke University.

1. Marx V (2005) Watching peptide drugs grown up. *Chem Eng News* 83(11):17–24.
2. Edwards CMB, Cohen MA, Bloom SR (1999) Peptides as drugs. *QJM* 92(1):1–4.
3. Niu CH, Chiu YY (1998) FDA perspective on peptide formulation and stability issues. *J Pharm Sci* 87(11):1331–1334.
4. Banga AK (2005) *Parenteral Controlled Delivery and Pharmacokinetics of Therapeutic Peptides and Proteins. Therapeutic Peptides and Proteins* (CRC, Boca Raton, FL), pp 177–227.
5. Meyer DE, Chilkoti A (2004) Quantification of the effects of chain length and concentration on the thermal behavior of elastin-like polypeptides. *Biomacromolecules* 5(3):846–851.
6. Hays NP, Galassetti PR, Coker RH (2008) Prevention and treatment of type 2 diabetes: Current role of lifestyle, natural product, and pharmacological interventions. *Pharmacol Ther* 118(2):181–191.
7. Hinnen D, Nielsen LL, Waninger A, Kushner P (2006) Incretin mimetics and DPP-IV inhibitors: New paradigms for the treatment of type 2 diabetes. *J Am Board Fam Med* 19(6):612–620.
8. Brubaker PL (2010) Minireview: Update on incretin biology: Focus on glucagon-like peptide-1. *Endocrinology* 151(5):1984–1989.
9. Nauck MA (1998) Glucagon-like peptide 1 (GLP-1): A potent gut hormone with a possible therapeutic perspective. *Acta Diabetol* 35(3):117–129.
10. Defronzo RA (2009) Banting lecture. From the triumvirate to the ominous octet: A new paradigm for the treatment of type 2 diabetes mellitus. *Diabetes* 58(4):773–795.
11. Holst JJ, Vilsbøll T, Deacon CF (2009) The incretin system and its role in type 2 diabetes mellitus. *Mol Cell Endocrinol* 297(1-2):127–136.
12. Brubaker PL, Drucker DJ (2004) Minireview: Glucagon-like peptides regulate cell proliferation and apoptosis in the pancreas, gut, and central nervous system. *Endocrinology* 145(6):2653–2659.
13. LeRoith D, Taylor SI, Olefsky JM (2004) *Diabetes Mellitus: A Fundamental and Clinical Text* (Lippincott Williams & Wilkins, Philadelphia), 3rd Ed, p xviii, 1540 pp.
14. Miranda LP, et al. (2008) Design and synthesis of conformationally constrained glucagon-like peptide-1 derivatives with increased plasma stability and prolonged in vivo activity. *J Med Chem* 51(9):2758–2765.
15. Fineman MS, Shen LZ, Taylor K, Kim DD, Baron AD (2004) Effectiveness of progressive dose-escalation of exenatide (exendin-4) in reducing dose-limiting side effects in subjects with type 2 diabetes. *Diabetes Metab Res Rev* 20(5):411–417.
16. Madsbad S, et al. (2011) An overview of once-weekly glucagon-like peptide-1 receptor agonists—Available efficacy and safety data and perspectives for the future. *Diabetes Obes Metab* 13(5):394–407.
17. Meyer DE, Chilkoti A (2002) Genetically encoded synthesis of protein-based polymers with precisely specified molecular weight and sequence by recursive directional ligation: Examples from the elastin-like polypeptide system. *Biomacromolecules* 3(2):357–367.
18. Trabbic-Carlson K, Liu L, Kim B, Chilkoti A (2004) Expression and purification of recombinant proteins from Escherichia coli: Comparison of an elastin-like polypeptide fusion with an oligohistidine fusion. *Protein Sci* 13(12):3274–3284.
19. Baggio LL, Drucker DJ (2007) Biology of incretins: GLP-1 and GIP. *Gastroenterology* 132(6):2131–2157.
20. Knudsen LB (2004) Glucagon-like peptide-1: The basis of a new class of treatment for type 2 diabetes. *J Med Chem* 47(17):4128–4134.
21. Amiram M, Quiroz FG, Callahan DJ, Chilkoti A (2011) A highly parallel method for synthesizing DNA repeats enables the discovery of 'smart' protein polymers. *Nat Mater* 10(2):141–148.
22. Yi L, Yin X, Wei D, Ma Y (2006) Expression and purification of exendin-4 dimer in Escherichia coli and its interaction with GLP-1 receptor in vitro. *Protein Pept Lett* 13(8):823–827.
23. Betre H, Setton LA, Meyer DE, Chilkoti A (2002) Characterization of a genetically engineered elastin-like polypeptide for cartilaginous tissue repair. *Biomacromolecules* 3(5):910–916.
24. Christensen T, et al. (2009) Fusion order controls expression level and activity of elastin-like polypeptide fusion proteins. *Protein Sci* 18(7):1377–1387.
25. Kim Y, et al. (1994) FT-IR and near-infrared FT-Raman studies of the secondary structure of insulinotropin in the solid state: Alpha-helix to beta-sheet conversion induced by phenol and/or by high shear force. *J Pharm Sci* 83(8):1175–1180.
26. Hupe-Sodmann K, et al. (1995) Characterisation of the processing by human neutral endopeptidase 24.11 of GLP-1(7-36) amide and comparison of the substrate specificity of the enzyme for other glucagon-like peptides. *Regul Pept* 58(3):149–156.
27. Kim JG, et al. (2003) Development and characterization of a glucagon-like peptide 1-albumin conjugate: The ability to activate the glucagon-like peptide 1 receptor in vivo. *Diabetes* 52(3):751–759.
28. Wang Q, et al. (2010) Novel GLP-1 fusion chimera as potent long acting GLP-1 receptor agonist. *PLoS ONE* 5(9):e12734.
29. Schellenberger V, et al. (2009) A recombinant polypeptide extends the in vivo half-life of peptides and proteins in a tunable manner. *Nat Biotechnol* 27(12):1186–1190.
30. Diamant M, et al. (2010) Once weekly exenatide compared with insulin glargine titrated to target in patients with type 2 diabetes (DURATION-3): An open-label randomised trial. *Lancet* 375(9733):2234–2243.
31. Kwak HH, et al. (2009) Pharmacokinetics and efficacy of a biweekly dosage formulation of exenatide in Zucker diabetic fatty (ZDF) rats. *Pharm Res* 26(11):2504–2512.
32. Shive MS, Anderson JM (1997) Biodegradation and biocompatibility of PLA and PLGA microspheres. *Adv Drug Deliv Rev* 28(1):5–24.
33. Pai SS, Tilton RD, Przybycien TM (2009) Poly(ethylene glycol)-modified proteins: Implications for poly(lactide-co-glycolide)-based microsphere delivery. *AAPS J* 11(1):88–98.
34. Burcelin R, Dolci W, Thorens B (1999) Long-lasting antidiabetic effect of a dipeptidyl peptidase IV-resistant analog of glucagon-like peptide-1. *Metabolism* 48(2):252–258.
35. Greenfield NJ (2006) Using circular dichroism spectra to estimate protein secondary structure. *Nat Protoc* 1(6):2876–2890.
36. Baggio LL, Huang Q, Brown TJ, Drucker DJ (2004) A recombinant human glucagon-like peptide (GLP)-1-albumin protein (albugon) mimics peptidergic activation of GLP-1 receptor-dependent pathways coupled with satiety, gastrointestinal motility, and glucose homeostasis. *Diabetes* 53(9):2492–2500.
37. Surwit RS, Kuhn CM, Cochrane C, McCubbin JA, Feinglos MN (1988) Diet-induced type II diabetes in C57BL/6J mice. *Diabetes* 37(9):1163–1167.